Supporting Information

For

Prediction of Adsorption Properties of Cyclic Hydrocarbons in MOFs using DFT-Derived Force Fields

Jason A. Gee and David S. Sholl*

School of Chemical & Biomolecular Engineering, Georgia Institute of Technology,

Atlanta, GA, 30332-0100

*Corresponding author: david.sholl@chbe.gatech.edu

Table of Contents

GCMC Simulation Details S1

Force Field Parameters S2

Comparison of Sim. and Exp. Lattice Constants S6

Assessment of D3FF Transferability and Convergence S7

Additional Comparison of Sim. and Exp. Isotherms S9

Comparison of Contributions to Sim. Heats of Adsorption S13

Additional Comparison of Sim. and Exp. Heats of Adsorption in DMOF-1 ..... S15

GCMC Simulation Details

Our Grand Canonical Monte Carlo (GCMC) simulations were performed using the RASPA simulation code.[1] Our GCMC simulations used an equilibration (production) period of at least 2×10^5 (1×10^6) Monte Carlo (MC) cycles. Each MC cycle consisted of a trial insertion/deletion, translation or rotation with equal probability. The Lennard-Jones (L-J) potential was truncated at a spherical cutoff distance of 13 Å. The L-J interaction parameters and charges for the adsorbate and framework atoms are provided in the next section. The cross-terms for the generic force fields were obtained using the Lorentz-Berthelot mixing rules. The Coulombic interactions were evaluated using the Ewald summation technique with a relative tolerance of 10^{-6}. The bulk fluid fugacity was assumed to be equal to the pressure in our calculations due to the low pressures examined in our study. For our binary mixture adsorption simulations the GCMC simulations included an additional MC move for exchanging adsorbed molecules to improve convergence. For these simulations, the adsorption selectivity was calculated using:

$$S_{ads} = \frac{q_1/q_2}{f_1/f_2} \tag{1}$$

where q_i (f_i) is the amount adsorbed (bulk fluid fugacity) of component i.

Force Field Parameters

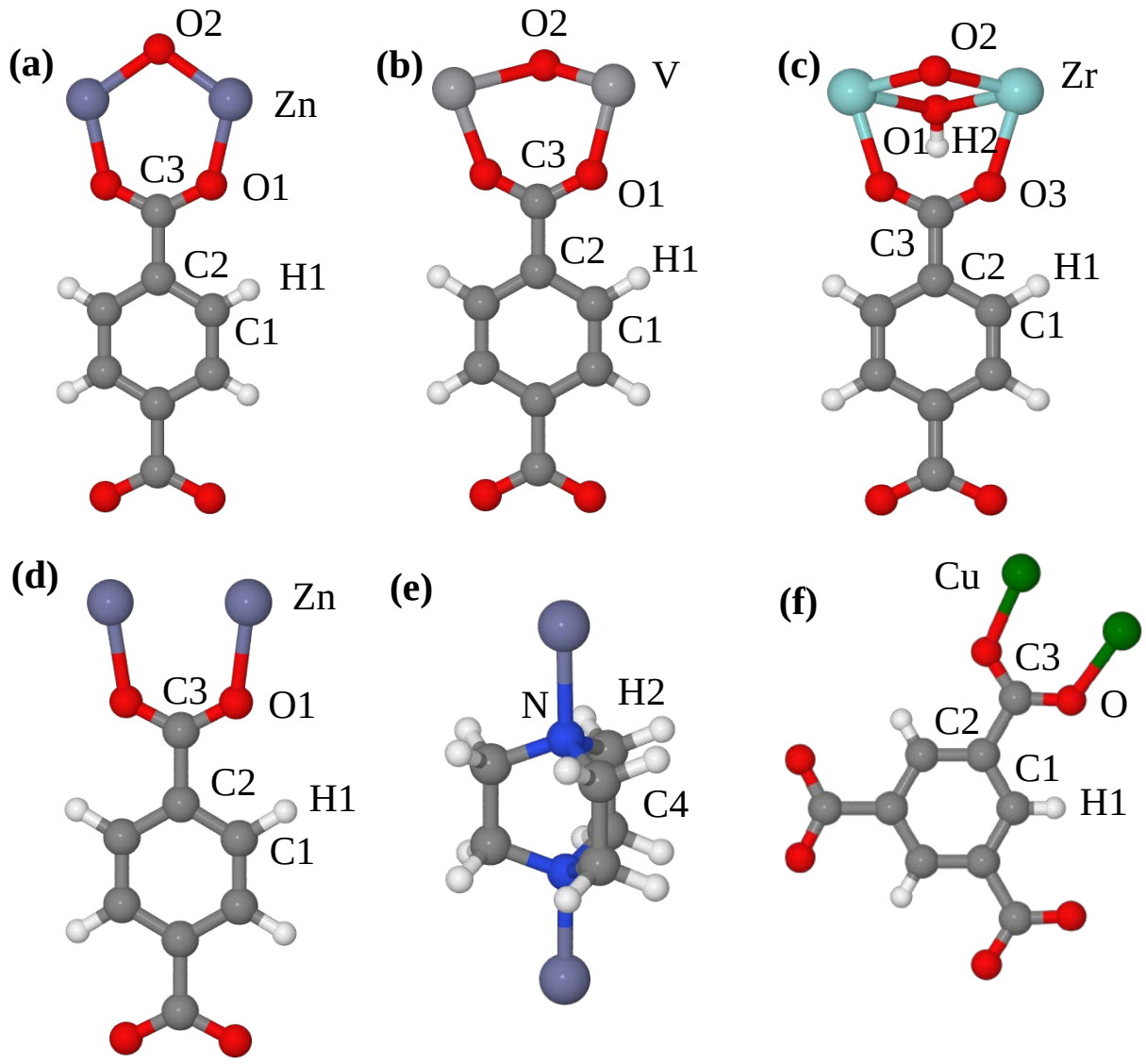

Figure S1. Atomic types of (a) IRMOF-1, (b) MIL-47, (c) UiO-66, (d) 1,4-benzene dicarboxylic acid (BDC), (e) 1,4-diazabicyclo[2.2.2]octane (DABCO) linker of DMOF-1, and (f) Cu-BTC.

Table S1. Atomic Charges for all MOFs Calculated Using the DDEC method.[2]

Atom Type	IRMOF-1	MIL-47	UiO-66	DMOF-1	Cu-BTC[3]
C1	-0.078000	-0.078990	-0.076220	-0.083401	-0.122900
C2	-0.091000	-0.091230	-0.103901	-0.078222	-0.007900
C3	0.698000	0.702750	0.746944	0.663467	0.650000
C4	-	-	-	-0.075150	-
H1	0.121000	0.120180	0.118463	0.103696	0.133900
H2	-	-	0.480712	0.098496	-
O1	-0.614000	-0.634790	-1.229380	-0.588859	-0.543600
O2	-1.262000	-0.793090	-1.237275	-	-
O3	-	-	-0.676147	-	-
N	-	-	-	-0.129068	-
Zn	1.118000	-	-	0.867308	-
V	-	1.944450	-	-	-
Zr	-	-	2.573494	-	-
Cu	-	-	-	-	0.868200

Table S2. Generic Force Field Lennard-Jones Parameters for MOFs.

Atom Type	UFF[4]		DREIDING[5]	
	ε/k_B (K)	σ (Å)	ε/k_B (K)	σ (Å)
C	52.87	3.43	47.89	3.47
H	22.16	2.57	7.65	2.85
O	30.21	3.12	48.19	3.03
N	34.75	3.26	38.97	3.26
Zn	62.44	2.46	27.69	4.05
V	8.06	2.80	-	-
Zr	34.75	2.78	-	-
Cu	2.52	3.11	-	-

Table S3. OPLS Force Field[6] Lennard-Jones Parameters for Cyclic Hydrocarbons.

Atom Type	ε/k_B (K)	σ (Å)	q (e)
C_aro	35.24	3.55	-0.115
H_aro	15.03	2.42	0.115
CH_3_xyl	85.51	3.80	0.115
CH_2_xyl	46.0	3.95	0.115
CH_3_sp^3	98.0	3.75	0.0

Table S4. D3FF Force Field Lennard-Jones Parameters for Cyclic Hydrocarbons.

Cross-species	ε/k_B (K)	σ (Å)
C_aro-C_frame	44.070	3.437
C_aro-H_frame	27.211	2.878
C_aro-O_frame	105.167	3.095
C_ R-C_frame	14.172	3.412
C_ R-H_frame	1.158	4.128
C_ R-O_frame	5.712	3.539
CH_3_xyl-C_frame	73.942	3.567
CH_3_xyl-H_frame	33.035	3.036
CH_3_xyl-O_frame	115.901	3.332
H_aro-C_frame	10.051	2.997
H_aro-H_frame	100.496	2.027
H_aro-O_frame	1.884	3.294

Figure S2. Atomic types for the xylene isomers.

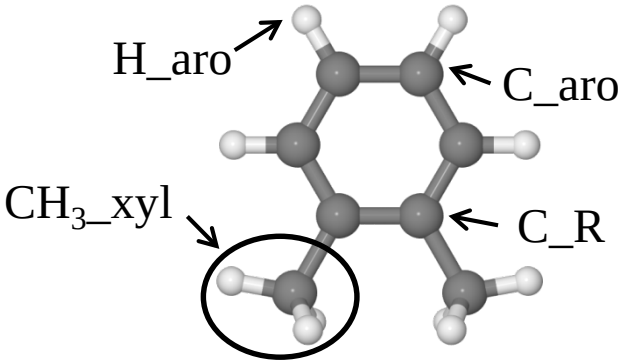

Comparison of Simulated and Experimental Lattice Constants

Table S5. Comparison of the Structural Parameters for MIL-47, DMOF-1, UiO-66, and IRMOF-1 from DFT Calculations and Experiments.

MOF	Lattice parameter (Å)		
	a	**b**	**c**
MIL-47 (DFT)	6.79	16.64	13.37
MIL-47 (exp.)[7]	6.81	16.41	13.57
DMOF-1 (DFT)	11.05	11.05	9.58
DMOF-1 (exp.)[8]	10.93	10.93	9.61
UiO-66 (prim., DFT)	14.79	14.79	14.79
UiO-66 (prim., exp.)[9]	14.80	14.80	14.80
IRMOF-1 (prim., DFT)	18.45	18.45	18.45
IRMOF-1 (prim., exp.)[10]	18.27	18.27	18.27

Note: DFT energy-minimizations of the framework atoms were performed with the DFT-D2 method because structural optimization with DFT-D3 was not implemented in the version of VASP used in our study.

Assessment of D3FF Transferability and Convergence

A critical test of the performance of D3FF is its transferability to other MOFs. To test this aspect of our fitting procedure, we performed an analysis of the number of materials in the test set required to accurately describe adsorption data in 1,200 configurations in all four materials we considered (MIL-47, DMOF-1, UiO-66, IRMOF-1). The force field developed using adsorption data in MIL-47 alone as the test set gave a mean absolute deviation (MAD) of 3.59 kJ/mol compared to DFT-D3. This value is within ~0.5 kJ/mol of the MAD obtained using D3FF, which was developed using 1,200 configurations in all four materials in its test set. A similar result was found using the adsorption data in other MOFs as the test set (data not shown). Based on this analysis, we conclude that our method is transferable to other MOF materials despite the small number of MOFs used in our test set.

In our fitting procedure described in the main text, we were only able to probe a limited number of configurations of the xylene isomers due to the computational cost of the single point DFT energy calculations. Therefore, it was necessary to determine the required number of configurations required to obtain a force field that is converged relative to the DFT data. To test the convergence of D3FF, we calculated the isosteric heat of adsorption of *o*-xylene (Q_{st}^{0}) versus the number of configurations used in the parameterization for all four materials in our test set. Our results in Figure S3 indicate that the Q_{st}^{0} are converged for these materials after ~300 configurations. As a result, we used this number of configurations in our final parameterization procedure to ensure that the D3FF is consistent with the DFT data.

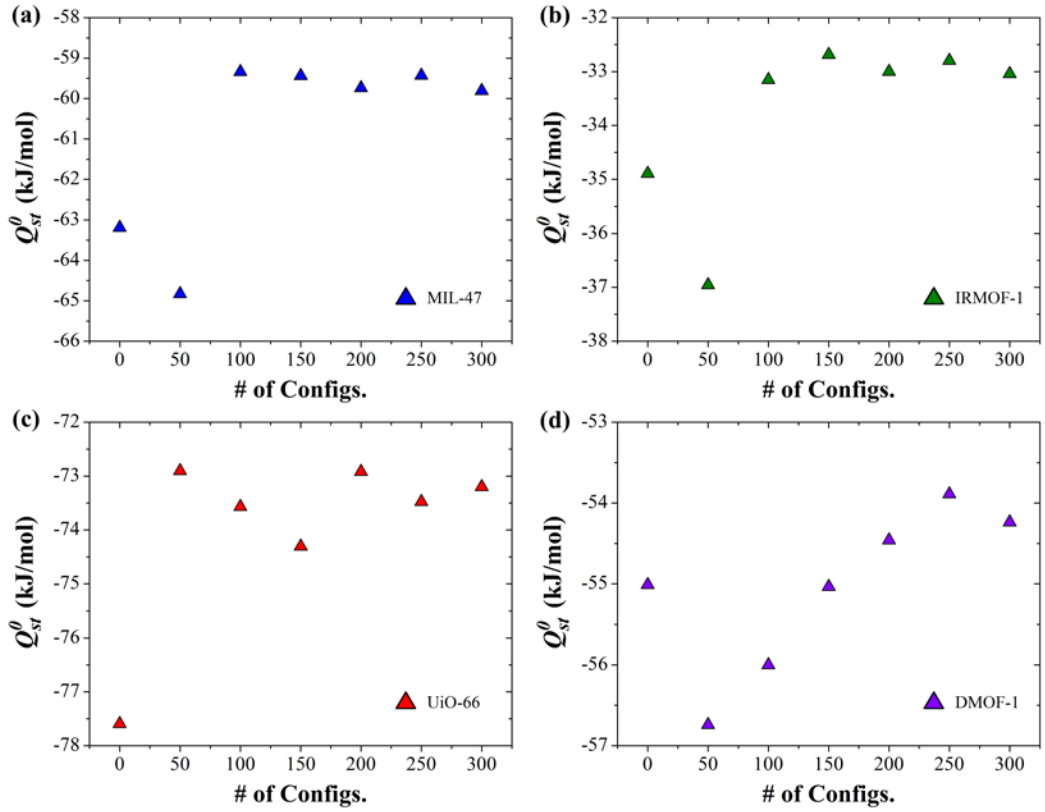

Figure S3. Simulated heat of adsorption of *o*-xylene at infinite dilution (Q_{st}^{0}) versus number of configurations used in our force field parameterization.

Additional Comparison of Sim. and Exp. Isotherms

In the main text, we showed a comparison of simulated and experimental adsorption isotherms. We noted that the simulated isotherms were scaled to approximately match the experimental saturation loadings for the purpose of comparison. Figure S4 shows a comparison of the scaled and un-scaled simulated isotherms to the experimental data. We found that scaling the simulated isotherms for DREIDING by 85% (60%) and D3FF by 80% (60%) for MIL-47 (DMOF-1) gave better agreement with the experimental saturation loadings. Therefore, this scaling was used to compare the simulated and experimental adsorption isotherm data in the main text.

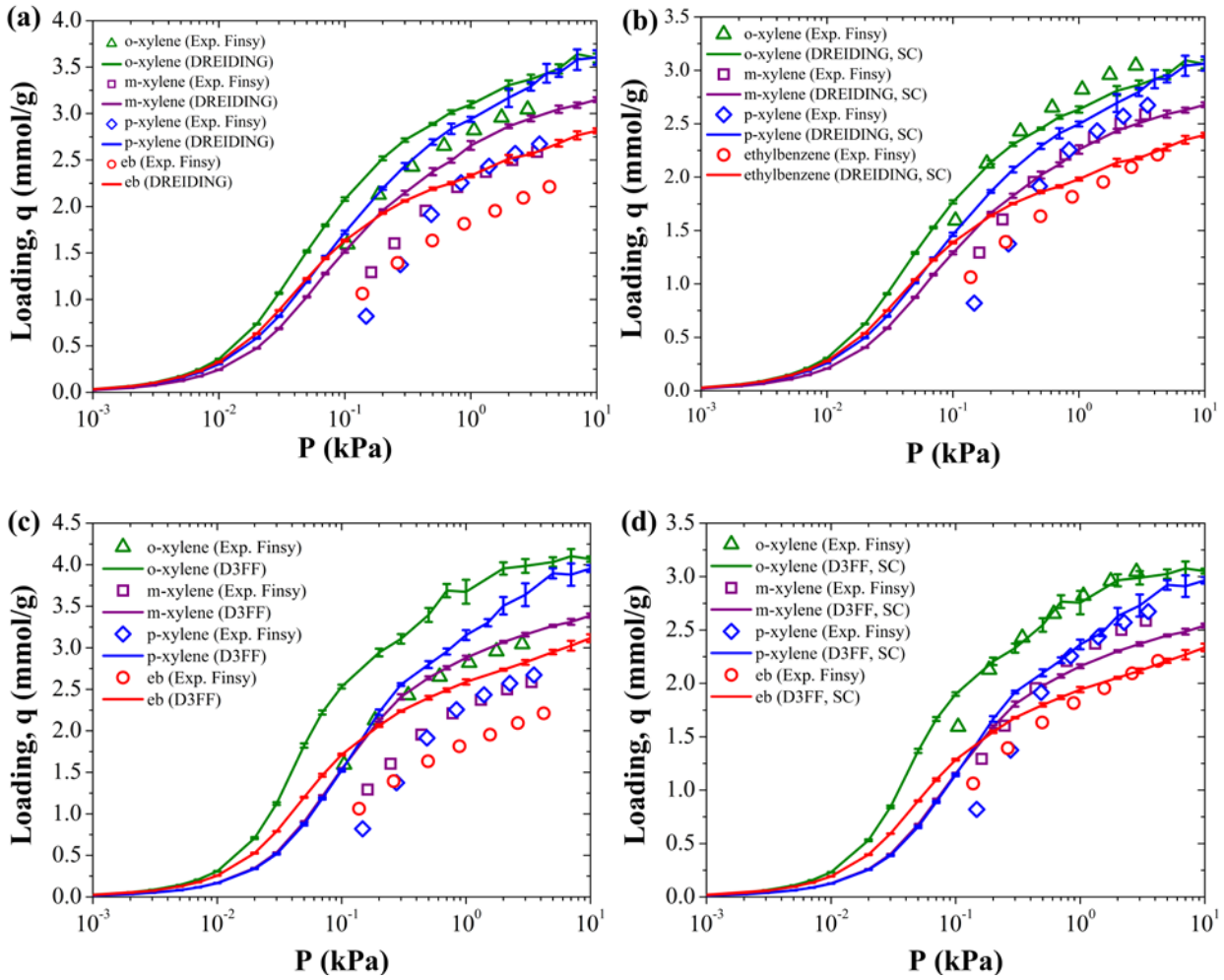

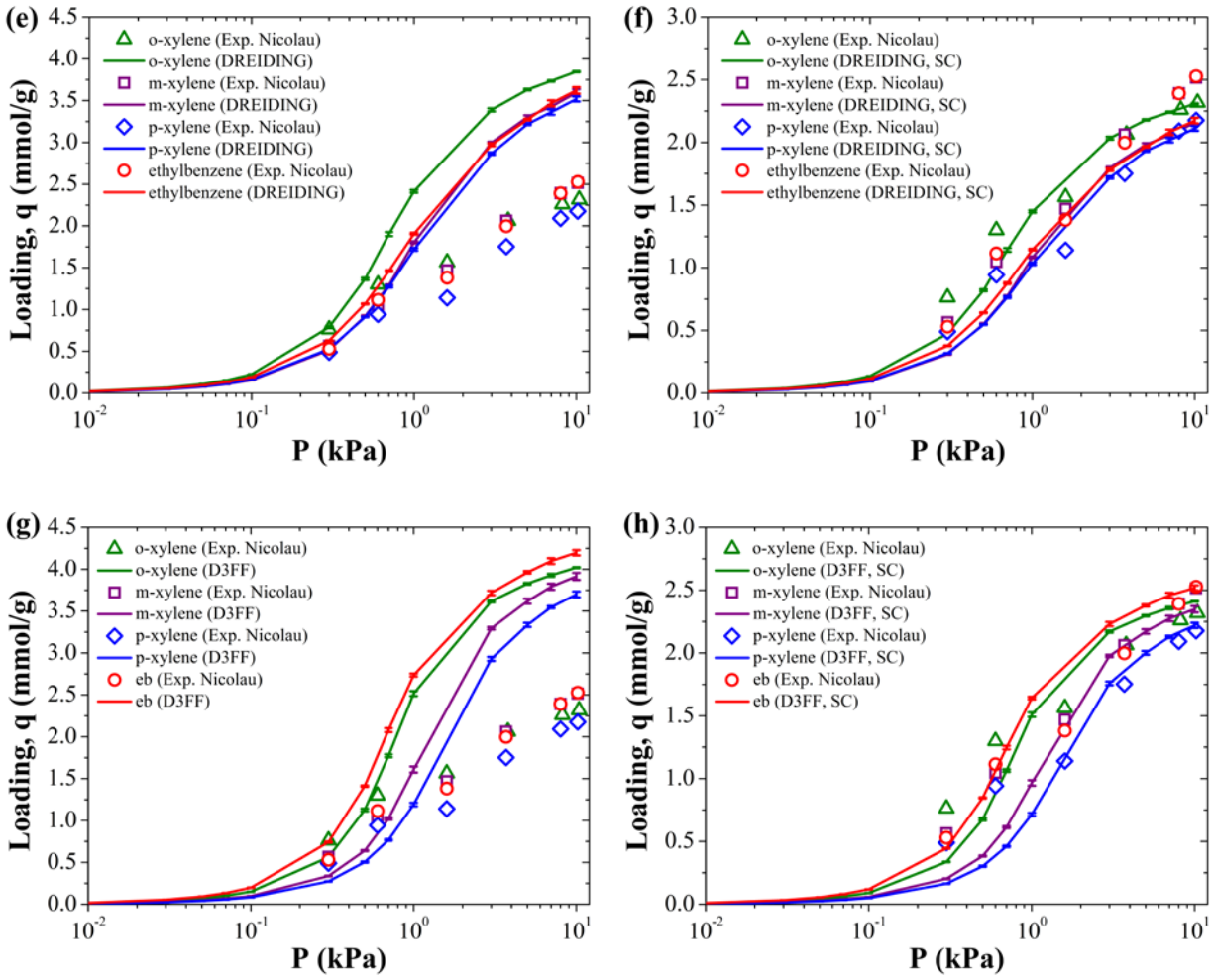

Figure S4. Comparison of scaled and un-scaled isotherms for xylene isomers using DREIDING (a,b) and D3FF (c,d) in MIL-47 at T = 423 K and DMOF-1 (e-h) at T = 448 K (c,d), respectively. The experimental data for MIL-47 and DMOF-1 are from Finsy et al.[11] and Nicolau et al.[12]

In the main text, we demonstrated that both generic and DFT-based force fields are able to capture the trends in adsorption uptake at a single temperature. It is also important to compare the adsorption uptake as a function of temperature to assess the transferability of the force fields to different operating conditions. In Figure S5, we demonstrate that both the generic and D3FF are able to accurately capture the experimental data at various temperatures for MIL-47 and DMOF-1. We should also note that both DREIDING and D3FF give a moderate deviation to

experimental data for the highest temperature in DMOF-1. It is unclear whether this discrepancy is due to inaccuracy of the force field or experimental uncertainty.

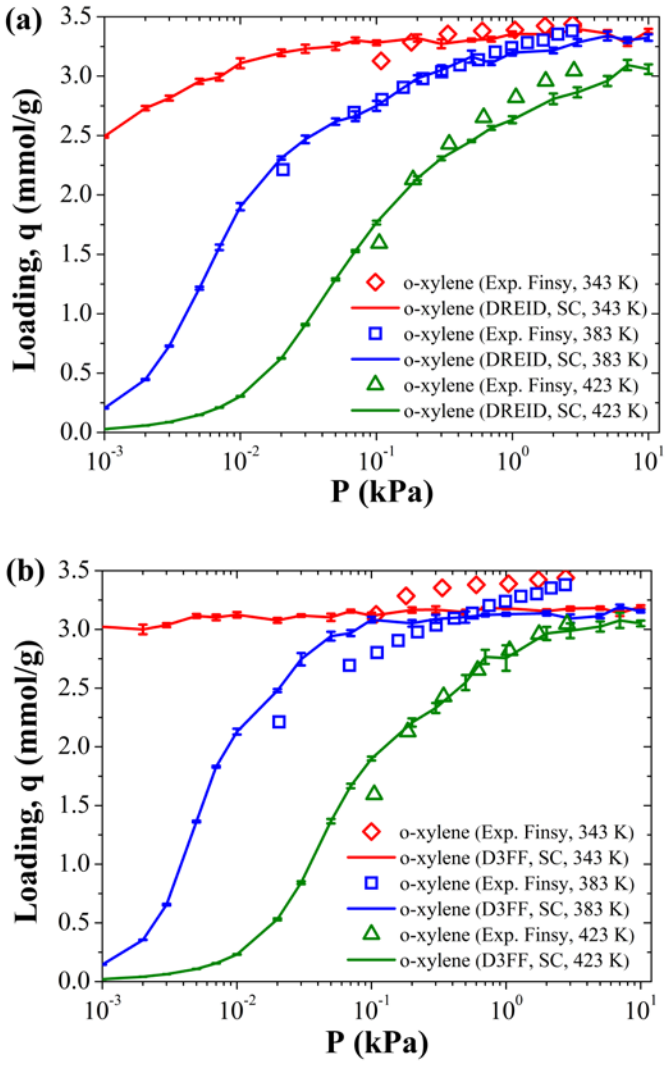

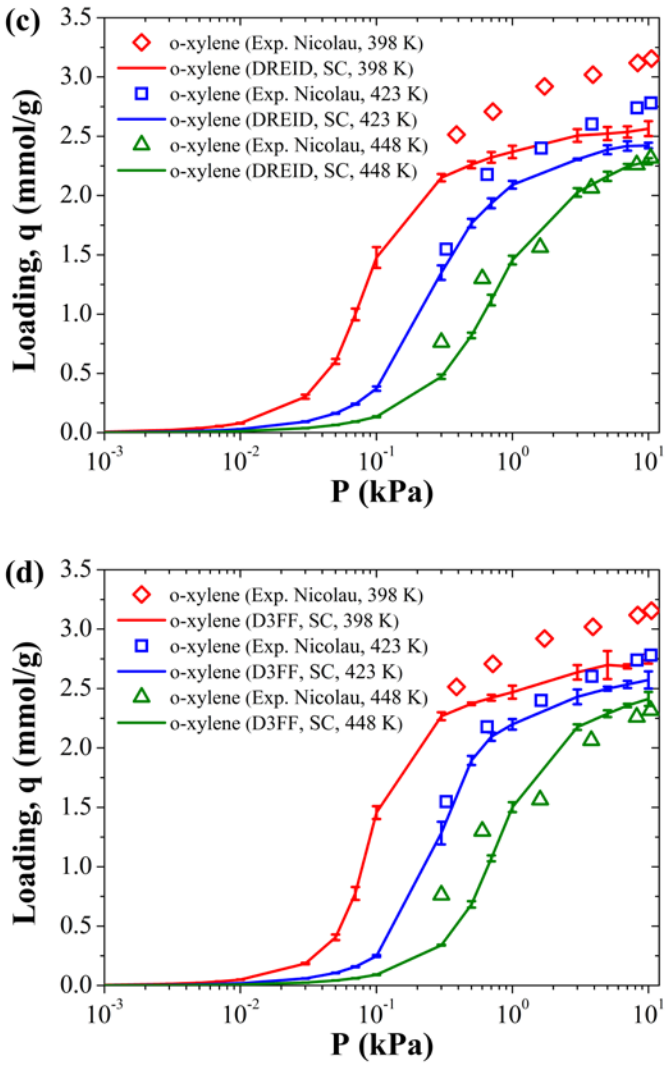

Figure S5. Comparison of the temperature dependence of simulated and experimental isotherms for xylene isomers using DREIDING and D3FF in MIL-47 (a,b) and DMOF-1 (c,d), respectively. The simulated isotherms are scaled to match the saturation loadings of the experimental isotherms at T = 423 K and T = 448 K in MIL-47 and DMOF-1, respectively, for the purpose of comparison.

Comparison of Contributions to Sim. Heats of Adsorption

In Figure 3 of the main text, we showed that the heat of adsorption versus loading for *ortho*-xylene showed different trends depending on the MOF under study. In Figure S6, we provide a breakdown of the contributions to the total heat of adsorption from host-guest and guest-guest interactions. The trend we observe in this figure is that the heat of adsorption versus loading is dominated by guest-guest interactions in the case of MIL-47 and host-guest interactions in UiO-66. This difference can be explained by a confining effect of the smaller cages in UiO-66. These cages have a large heat of adsorption at infinite dilution (Q_{st}^{0}) of ~75 kJ/mol and can only accommodate a single adsorbed xylene molecule. The xylenes adsorbed in these cages are unable to interact with other adsorbates due to the large separation between adjacent cages. Therefore, at low loadings the xylenes exhibit a small guest-guest contribution to the isosteric heat of adsorption (Q_{st}). At higher loadings, the total Q_{st} is reduced by adsorption in the larger cages and the guest-guest contribution becomes more significant, similar to MIL-47 and the other large-pore MOFs examined in our study.

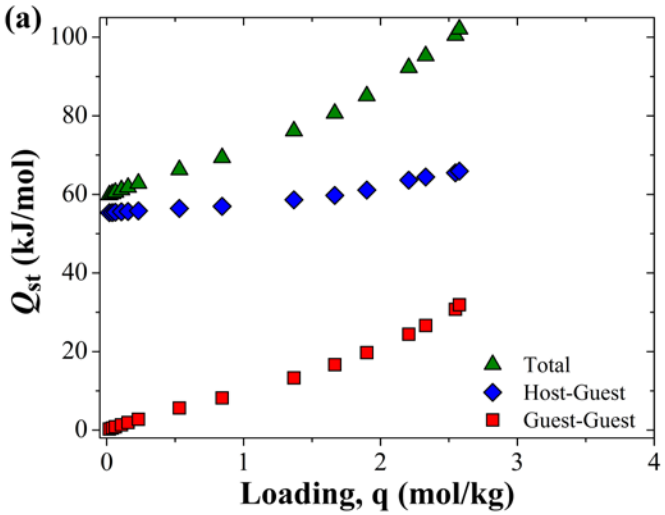

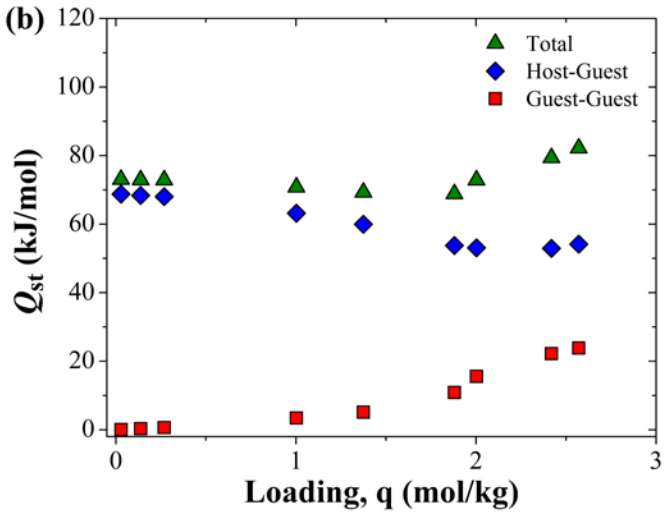

Figure S6. Comparison of the different contributions to the total heat of adsorption of *o*-xylene calculated using GCMC (D3FF) in (a) MIL-47 at T = 543 K and (b) UiO-66 at T = 423 K.

Note: Q_{st} is defined as:[13]

$$Q_{st} = \mathrm{RT} - \frac{\langle NU \rangle - \langle N \rangle \langle U \rangle}{\langle N^2 \rangle - \langle N \rangle^2} \qquad (1)$$

where N is the number of adsorbates, U is the potential energy, and "<…>" denotes an ensemble average. U can be partitioned into framework-adsorbate and adsorbate-adsorbate contributions. We did not include the "RT" term in the framework-adsorbate and adsorbate-adsorbate contributions to Q_{st} to avoid double-counting this contribution to the total Q_{st}. Therefore, the sum of these two contributions does not equal the total Q_{st} in these plots.

Additional Comparison of Sim. and Exp. Heats of Adsorption in DMOF-1

In the main text, we compared our simulated Q_{st}^{0} with experimental values reported by Nicolau et al.[12] for the xylene isomers and ethylbenzene in DMOF-1 using the Clasius-Clapeyron equation. In our work, we calculated the Q_{st} over the entire range of loadings using GCMC simulations. In Figure S7, we compare our results for the Q_{st} from GCMC simulations to the data reported by Nicolau et al. We find that the Q_{st}^{0} in this system cannot be measured based on adsorption data at high loadings as assumed in their work because of the presence of strong guest-guest interactions that are absent at low loadings. We also compared our GCMC simulation data to the Dual-Site Langmuir (DSL) fits of the experimental adsorption data of Nicolau et al. by Barcía et al.[14] We find that the DSL model cannot correctly capture the loading-dependence of the Q_{st} because it violates the assumption of non-interacting adsorbed molecules in the Langmuir adsorption model. We should also note that the GCMC data for the guest-framework contribution to the clearly shows that only a single adsorption site is present for the xylene isomers in DMOF-1.

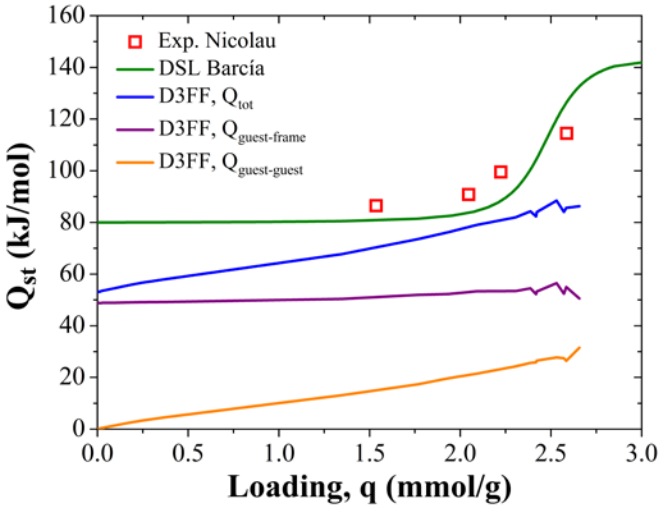

Figure S7. Comparison of heats of adsorption from experimental isotherm data of Nicolau et al.,[12] Dual-Site Langmuir (DSL) fits to the experimental data from Barcía et al,[14] and GCMC simulations (D3FF) for *o*-xylene in DMOF-1 at T = 423 K. The different contributions to the heats of adsorption calculated using D3FF are shown for comparison.

SUPPORTING INFORMATION REFERENCES

(1) Dubbeldam, D.; Calero, S.; Ellis, D.; Snurr, R. RASPA 1.0. *Northwestern University: Evanston, IL* **2008**.

(2) Manz, T. A.; Sholl, D. S. Improved Atoms-in-Molecule Charge Partitioning Functional for Simultaneously Reproducing the Electrostatic Potential and Chemical States in Periodic and Nonperiodic Materials. *Journal of Chemical Theory and Computation* **2012**, *8*, 2844-2867.

(3) Zang, J.; Nair, S.; Sholl, D. S. Prediction of Water Adsorption in Copper-Based Metal–Organic Frameworks Using Force Fields Derived from Dispersion-Corrected DFT Calculations. *The Journal of Physical Chemistry C* **2013**, *117*, 7519-7525.

(4) Rappe, A. K.; Casewit, C. J.; Colwell, K. S.; Goddard, W. A.; Skiff, W. M. UFF, a full periodic table force field for molecular mechanics and molecular dynamics simulations. *Journal of the American Chemical Society* **1992**, *114*, 10024-10035.

(5) Mayo, S. L.; Olafson, B. D.; Goddard, W. A. DREIDING: a generic force field for molecular simulations. *The Journal of Physical Chemistry* **1990**, *94*, 8897-8909.

(6) Jorgensen, W. L.; Laird, E. R.; Nguyen, T. B.; Tirado-Rives, J. Monte Carlo simulations of pure liquid substituted benzenes with OPLS potential functions. *Journal of Computational Chemistry* **1993**, *14*, 206-215.

(7) Alaerts, L.; Kirschhock, C. E. A.; Maes, M.; van der Veen, M. A.; Finsy, V.; Depla, A.; Martens, J. A.; Baron, G. V.; Jacobs, P. A.; Denayer, J. F. M., et al. Selective Adsorption and Separation of Xylene Isomers and Ethylbenzene with the Microporous Vanadium(IV) Terephthalate MIL-47. *Angewandte Chemie International Edition* **2007**, *46*, 4293-4297.

(8) Dybtsev, D. N.; Chun, H.; Kim, K. Rigid and Flexible: A Highly Porous Metal–Organic Framework with Unusual Guest-Dependent Dynamic Behavior. *Angewandte Chemie* **2004**, *116*, 5143-5146.

(9) Cavka, J. H.; Jakobsen, S.; Olsbye, U.; Guillou, N.; Lamberti, C.; Bordiga, S.; Lillerud, K. P. A New Zirconium Inorganic Building Brick Forming Metal Organic Frameworks with Exceptional Stability. *Journal of the American Chemical Society* **2008**, *130*, 13850-13851.

(10) Eddaoudi, M.; Kim, J.; Rosi, N.; Vodak, D.; Wachter, J.; O'Keeffe, M.; Yaghi, O. M. Systematic design of pore size and functionality in isoreticular MOFs and their application in methane storage. *Science* **2002**, *295*, 469-472.

(11) Finsy, V.; Verelst, H.; Alaerts, L.; De Vos, D.; Jacobs, P. A.; Baron, G. V.; Denayer, J. F. M. Pore-Filling-Dependent Selectivity Effects in the Vapor-Phase Separation of Xylene Isomers on the Metal−Organic Framework MIL-47. *Journal of the American Chemical Society* **2008**, *130*, 7110-7118.

(12) Nicolau, M. P.; Bárcia, P. S.; Gallegos, J. M.; Silva, J. A.; Rodrigues, A. E.; Chen, B. Single-and multicomponent vapor-phase adsorption of xylene isomers and ethylbenzene in a microporous metal− organic framework. *The Journal of Physical Chemistry C* **2009**, *113*, 13173-13179.

(13) Karavias, F.; Myers, A. L. Isosteric heats of multicomponent adsorption: thermodynamics and computer simulations. *Langmuir* **1991**, *7*, 3118-3126.

(14) Bárcia, P. S.; Guimarães, D.; Mendes, P. A. P.; Silva, J. A. C.; Guillerm, V.; Chevreau, H.; Serre, C.; Rodrigues, A. E. Reverse shape selectivity in the adsorption of hexane and xylene isomers in MOF UiO-66. *Microporous and Mesoporous Materials* **2011**, *139*, 67-73.